Journal of Alloys and Compounds 509 (2011) 4788–4792

Contents lists available at ScienceDirect

Journal of Alloys and Compounds

journal homepage: www.elsevier.com/locate/jallcom

Synthesis of tungsten oxide ($W_{18}O_{49}$) nanosheets utilizing EDTA salt by microwave irradiation method

V. Hariharan[a], M. Parthibavarman[a], C. Sekar[a,b,*]

[a] Centre for Nanoscience and Technology, Department of Physics, Periyar University, Salem 636 011, Tamilnadu, India
[b] Department of Bioelectronics and Biosensors, Alagappa University, Karaikudi 630 003, Tamilnadu, India

ARTICLE INFO

Article history:
Received 14 August 2010
Received in revised form 19 January 2011
Accepted 20 January 2011
Available online 3 February 2011

Keywords:
Tungsten oxide
Microwave irradiation
TEM analyses
EDTA

ABSTRACT

We report the synthesis of crystalline $W_{18}O_{49}$ with nanosheet like morphology by low cost microwave irradiation method without employing hydrothermal process for the first time. Initially, $WO_3 \cdot H_2O$ was synthesized using ethylenediaminetetraacetic acid (EDTA) as surface modulator. The product was annealed at 600 °C for 6 h in ambient atmosphere in order to obtain anhydrous tungsten oxide $W_{18}O_{49}$. Powder X-ray diffraction results confirmed the as prepared $WO_3 \cdot H_2O$ to be orthorhombic and $W_{18}O_{49}$ to be monoclinic phase, respectively. Transmission electron micrographs (TEM) revealed that the $W_{18}O_{49}$ nanosheets have the average dimensions of the order of 250 nm in length and around 150 nm in width. UV–visible diffusion reflectance spectroscopic (DRS) studies revealed the band gap energies to be 3.28 and 3.47 eV for $WO_3 \cdot H_2O$ and $W_{18}O_{49}$ samples, respectively. The growth mechanism of two dimensional $W_{18}O_{49}$ nanosheets is discussed.

1. Introduction

The nanostructured transition metal oxides (TMOs) have attracted considerable attention in the past decade because of their unique chemical and physical properties leading to numerous potential applications. Tungsten oxides ($WO_{3-\delta}$) represent a fascinating class of material used for flat panel devices [1], smart windows [2], anti glare mirrors [3], etc. because of its outstanding electro, photo and gas chromic properties. In particular, $W_{18}O_{49}$ has been explored for many applications such as gas sensors [4], photocatalysis [5], catalysis in electrochemical process [6], etc. Thus controlled production of WO_3 based nanostructures in the presence of surface modulators has become significant particularly due to their flexible processing chemistry [7]. Tungsten oxide nanoparticles have been prepared by diverse techniques like microwave hydrothermal method [8], surfactant mediated method [9], acidification method [10], precipitation method [11], etc. Among these, Jang-Hoon Ha et al. [8] have used EDTA as surface modulator to synthesize self assembled one dimensional hydrated WO_3 nanowire bundles by microwave hydrothermal process. The authors have concluded that the sodium ions from EDTA in the reaction medium plays a unique role even though the presence of ammonium ions is required for producing urchin like structure because of its highly ordered self assembled nature. Yuxiang Qin et al. [12] have reported the synthesis of one dimensional $W_{18}O_{49}$ and two dimensional WO_3 nanostructures by solvothermal method. The authors showed that the one dimensional $W_{18}O_{49}$ nanowire bundles have a much higher response value and faster response-recovery characteristics to NO_2 gas than WO_3. Deepa et al. [13] have derived crystalline oxygen deficient WO_3 by sol–gel method. Though the sol–gel method is simple and less time consuming, the products are predominantly amorphous with poor chemical stability and further heat treatment is necessary to enhance the crystallanity. Most of the above mentioned methods used for the synthesis of $W_{18}O_{49}$ are time consuming and expensive.

In this work, we report the rapid synthesis of $W_{18}O_{49}$ by microwave irradiation method with and without using EDTA salt as surfactant for the first time. In both the cases, time required for synthesis was around 10 min only and the reaction process was also very simple.

2. Experimental procedures

The precursor solution was prepared by dissolving 2.49 g of tungstic acid (H_2WO_4) in 10 ml of sodium hydroxide (NaOH). This resulted in yellow colored hydrated sodium tungstate solution due to proton exchange protocol process [14]. Subsequently 0.5 g of EDTA (i.e. ~20 wt.% of tungstic acid) was added to the precursor solution to act as a surfactant and several drops of HCl was introduced into the solution to attain the pH value of 1. HCl acts as a precipitating agent and also medium for the product to have desired morphology [15]. About 5 ml double distilled water (i.e. ~50 vol.% of precursor solution) was added with the above solution in order to respond to microwave quickly. The final solution was exposed to microwave (2.45 GHz) under optimum power of 180 W for 10 min in air atmosphere. After

* Corresponding author at: Department of Bioelectronics and Biosensors, Alagappa University, Karaikudi 630 003, Tamilnadu, India. Tel.: +91 94425 63637; fax: +91 4565 225202.
E-mail address: Sekar2025@gmail.com (C. Sekar).

0925-8388/$ – see front matter © 2011 Published by Elsevier B.V.
doi:10.1016/j.jallcom.2011.01.159

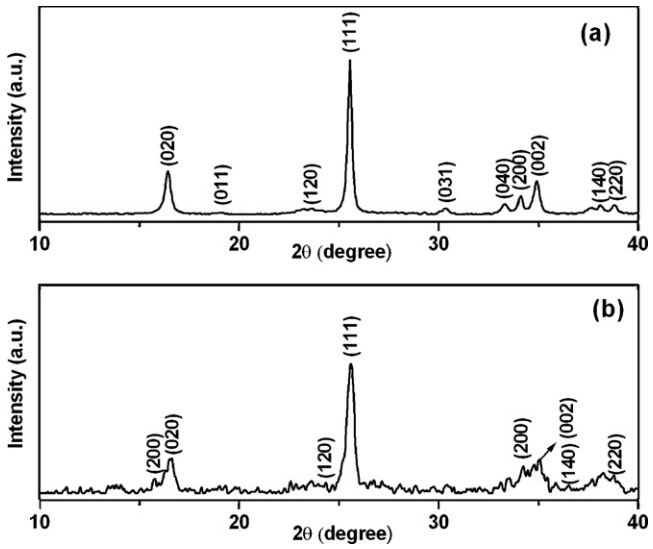

Fig. 1. Powder X-ray diffraction pattern of $WO_3 \cdot H_2O$ prepared (a) without and (b) with EDTA.

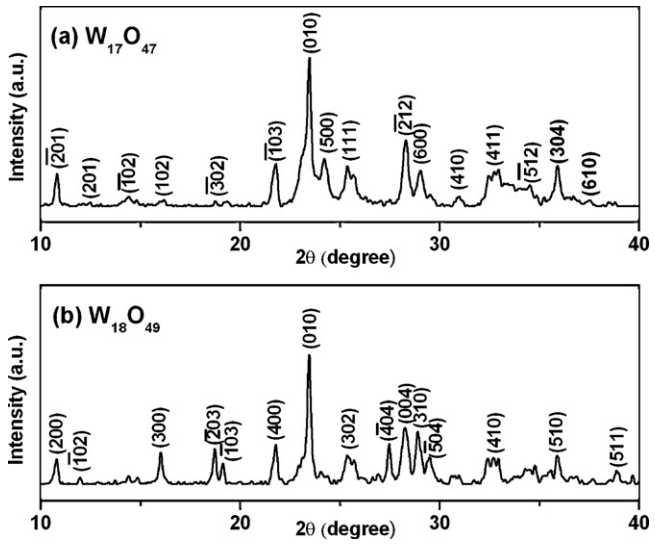

Fig. 2. Powder XRD pattern of the annealed samples (a) $W_{17}O_{47}$ (without EDTA) and (b) $W_{18}O_{49}$ (with EDTA).

irradiation a very small amount of surrounding water present in the product was removed by drying at 60 °C in air for 1 h. The above process was repeated without adding EDTA salt under the identical conditions. Both the products resulted in yellow colored powder which was annealed at 600 °C in air for 6 h to attain crystalline anhydrous tungsten oxide.

Thermal analysis was performed on SDT Q600 V8.3 Build 101. X-ray powder diffraction (XRD) patterns of all the samples were measured on a Bruker AXS D8 advanced diffractometer with monochromatic CuKα – radiation (λ = 1.5406 Å). TEM images and a Selected-area electron diffraction (SAED) were recorded on a Technai G20-stwin High resolution electron microscope (HRTEM) using an accelerating voltage of 200 kV. Optical properties were analyzed by UV–VIS diffusion reflectance spectroscopy using CARY 5E UV–VIS–NIR spectrophotometer (200–800 nm).

3. Results and discussion

3.1. Synthesis of WO_3

Hydrated tungsten oxide ($WO_3 \cdot H_2O$) was successfully synthesized by microwave irradiation method with and without using EDTA as surfactant. The reaction time required in both the cases was about 10 min only. The products were found to be pale yellow in colour. Powder XRD results confirmed the formation of orthorhombic phase of perovskite-like structure for both the samples prepared without EDTA (Fig. 1a) and with EDTA (Fig. 1b). All the diffraction peaks could be indexed as per the JCPDS data (43-0679) [16]. XRD pattern of $WO_3 \cdot H_2O$ prepared without EDTA revealed sharp and stronger peaks when compared to that of the sample prepared using the surfactant EDTA. The samples were annealed at 600 °C in air for 6 h in ambient atmosphere which resulted in oxygen deficient $WO_{3-\delta}$ phase.

The XRD pattern of annealed samples prepared with and without using EDTA could be assigned to $W_{17}O_{47}$ (JCPDS card-79-0171) (Fig. 2a) and $W_{18}O_{49}$ (JCPDS card-84-1516) (Fig. 2b) phases with monoclinic structures. The oxygen content of EDTA assisted sample was found to be slightly lower than that of the surfactant free sample. XRD pattern of EDTA assisted $W_{18}O_{49}$ sample contains more number of peaks and they are sharper when compared to that of the sample prepared without surfactant. Even though the positions of the diffractions peaks are identical, the orientations of planes for each case are different (see Fig. 2a and b). This is attributed to the fact that the structure variation between WO_3 and WO_2 leads to change in linking of coordination polyhedral from corner sharing to edge sharing [17]. Thus the presence of EDTA enhances the crystallinity and reduces the oxygen content of the end product. In general, tungsten oxides easily lose oxygen and are represented as $WO_{3-\delta}$. The oxidation state of tungsten in $W_{18}O_{49}$ lies between +4 (WO_2) and +6 (WO_3). With larger non-stoichiometry the defects preferentially accumulate at so called crystallographic shear planes along (*l*, *m*, 0) with the formation of edge-shared WO_6 octahedra [18]. The intensity at (0 1 0) reflection for both the samples is

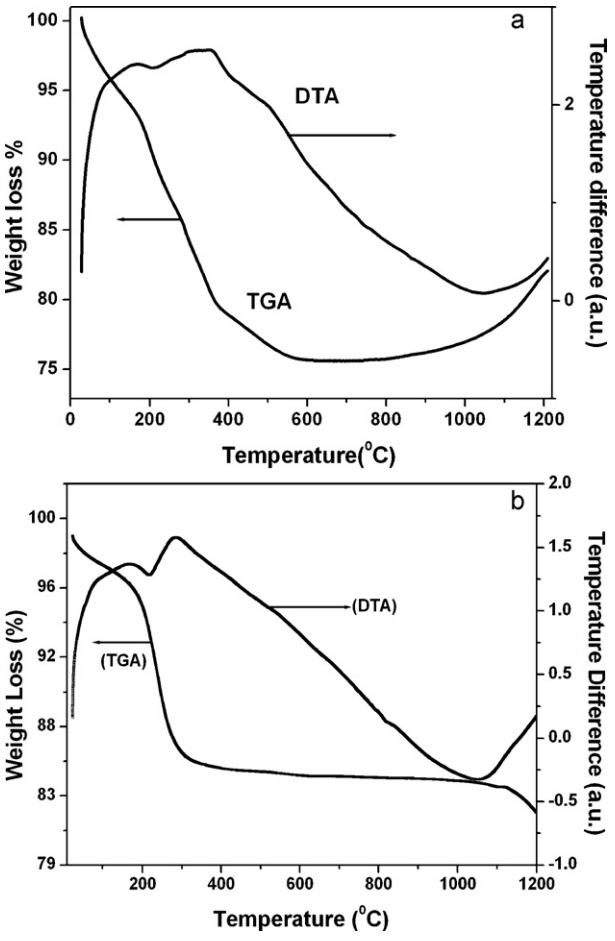

Fig. 3. TG–DTA curves of $WO_3 \cdot H_2O$ prepared (a) with EDTA and (b) without EDTA.

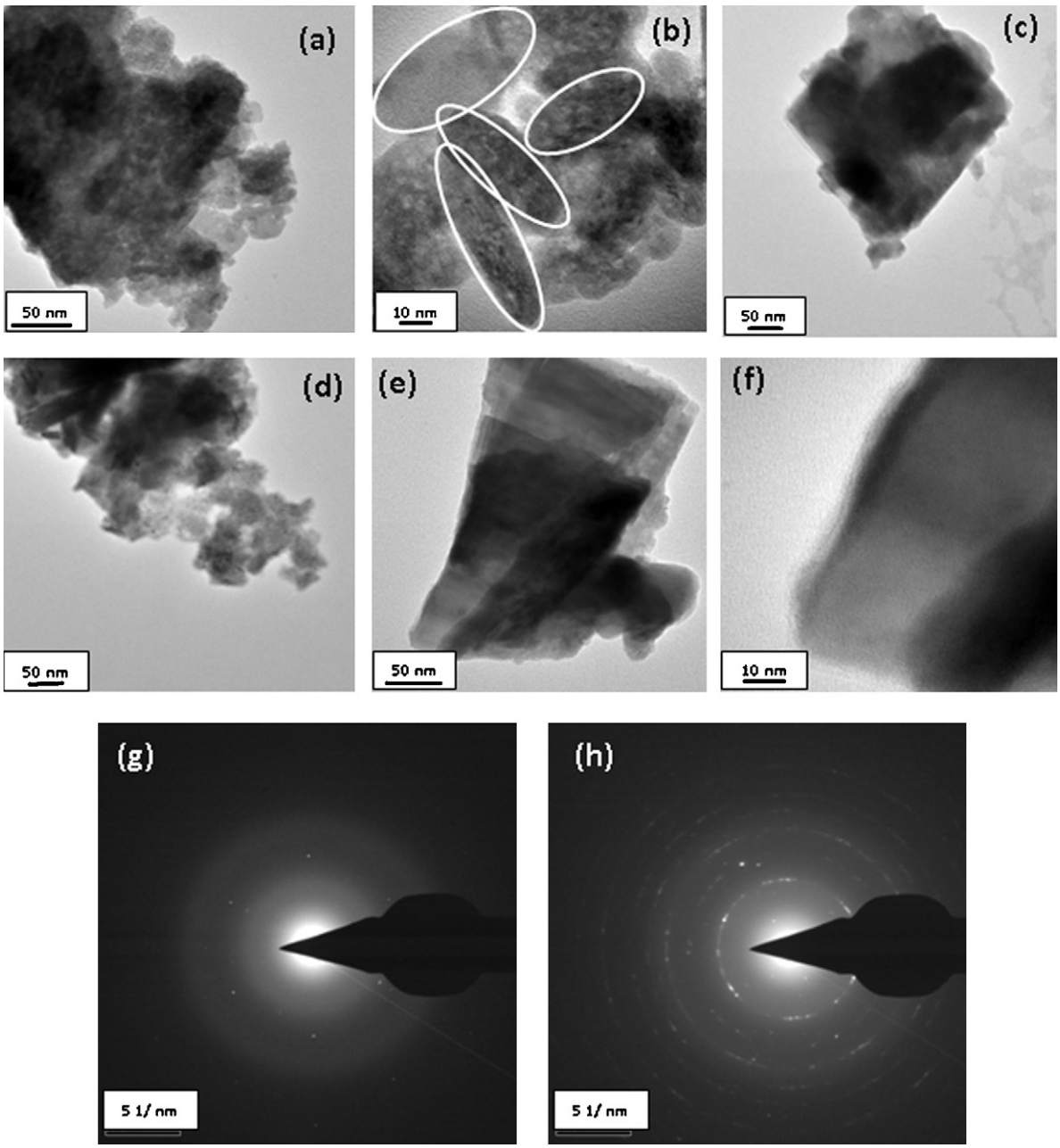

Fig. 4. TEM images of (a) $WO_3 \cdot H_2O$ without EDTA with low magnification. (b) $WO_3 \cdot H_2O$ without EDTA with high magnification. (c) $W_{17}O_{47}$ (annealed at 600 °C for 6 h in air ambient). (d) $WO_3 \cdot H_2O$ with EDTA. (e) $W_{18}O_{49}$ (annealed at 600 °C for 6 h) with EDTA – low magnification. (f) $W_{18}O_{49}$ (annealed at 600 °C for 6 h) with EDTA – high magnification. (g) SAED pattern of $WO_3 \cdot H_2O$ without EDTA. (h) SAED pattern of $W_{18}O_{49}$ (annealed at 600 °C for 6 h) with EDTA.

greater than other peaks suggesting that the crystalline $W_{17}O_{47}$ and $W_{18}O_{49}$ nanosheets were oriented along the (0 1 0) direction.

EDTA has been widely used as chelating agent and as surface modulator in the synthesis of many nanostructured materials [8]. The presence of sodium ion (Na^+) in EDTA plays a crucial role in modifying the morphology of the product by adsorbing oxygen quickly during the annealing process. Thus, it appears that Na^+ based EDTA salt has resulted self assembled tungsten oxide nanostructures [8]. In a similar work, we have prepared $WO_3 \cdot H_2O$ using PEG as surfactant. Subsequent annealing under identical conditions resulted in stoichiometric WO_3 which has been attributed to the absence of non adsorbing oxygen in PEG. On the other hand, annealing of $WO_3 \cdot H_2O$ prepared using EDTA resulted in oxygen deficient $W_{18}O_{49}$. This may be due to the formation of intermediate sodium oxide (Na_2O) during annealing process. The EDTA may also act as a driving force in producing such sheet like structure of $W_{18}O_{49}$ during annealing process.

3.2. Thermal analysis

TG–DTA curves of hydrated tungsten oxides prepared using with and without EDTA are shown in Fig. 3a and b, respectively. The data were recorded in air atmosphere in the temperature range 30–1100 °C with the heating rate of 20 °C per min. TG result of $WO_3 \cdot H_2O$ prepared using EDTA displays weight loss in four steps: first weight loss of 6.62 wt.% occurred up to 159 °C corresponds to the loss of interstitial water in $WO_3 \cdot H_2O$. The second weight loss of 7.82 wt.% up to 279 °C may be due to the loss of chemically bonded water and organic species such as carbon which is present from surface modulating agent (EDTA salt). The third and fourth

steps between 279 °C and 572 °C (6.11 wt.% and 3.89 wt.%) may be attributed to the removal of organic and inorganic species like carbonaceous compounds, sodium and chlorine ions which are present in the precursor solution from Na_2WO_4 and HCl. The observed weight gain above 800 °C indicates the possible oxygen uptake from ambient air which leads to stoichiometric tungsten oxide (WO_3). The DTA results indicate the two possible phase transitions around 356 °C and 503 °C, respectively. The exothermic peak at 356 °C corresponds to the phase transition of orthorhombic $WO_3{\cdot}H_2O$ into orthorhombic WO_3 (Space group: Pmnb). The other peak at 503 °C corresponds to the phase transition of orthorhombic WO_3 (Space group: Pmnb) to monoclinic $W_{18}O_{49}$ (Space group: P2/m). For comparison, the TG–DTA curves of $WO_3{\cdot}H_2O$ prepared without EDTA are shown in Fig. 3b. The total weight loss was found to be 13.31% which could be attributed to the loss of some physically adsorbed and chemically bonded water in addition to a small amount of inorganic species like sodium and chlorine ions. Thus the total weight loss (13.3%) is much less than that of the sample (25%) $WO_3{\cdot}H_2O$ prepared using EDTA. Further it can be noted that there was no oxygen uptake during high temperature treatment from 311 °C to 1100 °C. This clearly indicates that the surfactant play important role in fixing the oxygen content and stability of the end product.

3.3. TEM analyses

Fig. 4a and b shows the TEM micrographs of $WO_3{\cdot}H_2O$ synthesized without adding EDTA. Higher magnification (Fig. 4b) picture reveals that the sample consisted of nanosized tablets of different dimensions. Upon annealing at 600 °C in air for 6 h these tiny particles aggregated and resulted in platelet like morphology (Fig. 4c). Fig. 4d shows the TEM image of $WO_3{\cdot}H_2O$ prepared using EDTA. This sample is made up of nanosized crystals fairly well dispersed when compared to the sample grown without EDTA (Fig. 4a). Annealing this sample under identical conditions led to platelets which are made up of a number of nanosheets with dimensions of the order of about 250 nm in length and 150 nm in breadth (Fig. 4e). HRTEM image of EDTA assisted annealed sample $W_{18}O_{49}$ (Fig. 4f) reveal the d spacing of the lattice fringes to be around 0.5 nm which corresponds to (1 0 2) plan in XRD pattern. This indicate that the system is grown along *a* and *c* axes. The presence of sodium ion (Na^+) in EDTA salt absorbs oxygen during annealing process which might lead to the growth of two dimensional sheet like structure along *a* and *c* axes (1 0 2). It can be noticed that the width is half time than the length in agreement with the plane value. The selected area electron diffraction (SAED) pattern for $WO_3{\cdot}H_2O$ grown without EDTA (Fig. 4g) shows the single crystalline nature whereas annealed sample reveal the occurrence of a very uniform halo-ring shaped electron diffraction spots indicating poly crystalline nature of the sample (Fig. 4h).

3.4. FT-IR analyses

Fig. 5a and b shows the FT-IR spectra of $WO_3{\cdot}H_2O$ prepared using EDTA and annealed sample $W_{18}O_{49}$. respectively. The observed wave numbers, relative intensities obtained from the recorded spectra and the assignments were listed in Table 1. In both the samples, the frequency range between 900 and 600 cm^{-1} are clearly distinguished and are attributed to stretching (υ O–W–O) modes of WO_3 [19].

The bands present in the region 3100–3550 cm^{-1} belong to O–H stretching vibrations (asymmetric and symmetric) of coordinated water. The peaks at around 1595 cm^{-1} may be assigned to H–O–H bending of the coordinated water [20]. The additional peaks observed at 2822 cm^{-1} and 1352 cm^{-1} belong to CH_2 stretching, CH wagging vibration, respectively. It can be noticed that the peak intensity of the annealed sample ($W_{18}O_{49}$) is slightly weaker when compared to that of as prepared sample ($WO_3{\cdot}H_2O$). Although the TG results (heating rate 20 °C/min) suggest that the organic impurities are removed already at lower temperatures (Section 3.2), the high sensitive FT-IR results indicate the presence of some organic impurities in the product. Hence, we suggest that a prolonged annealing is required in order to remove all the organic species present in the samples.

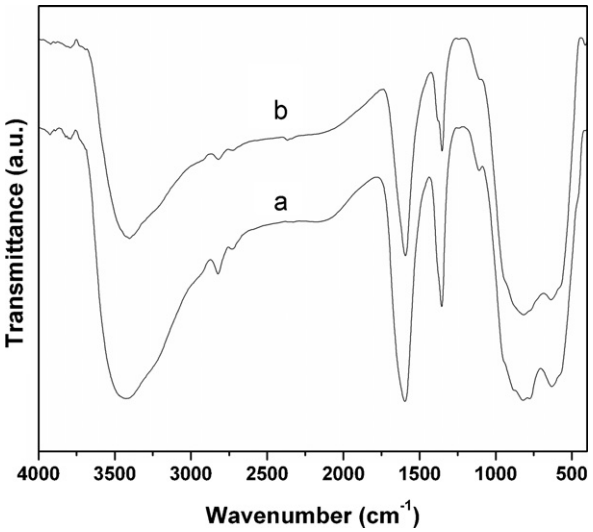

Fig. 5. FT-IR spectrum of (a) as prepared $WO_3{\cdot}H_2O$ and (b) $W_{18}O_{49}$ annealed at 600 °C. Both the samples were prepared using EDTA as surfactant.

3.5. UV–visible diffusion reflectance spectroscopy

Fig. 6 shows the diffusion reflectance spectra of EDTA assisted as prepared ($WO_3{\cdot}H_2O$) and annealed sample ($W_{18}O_{49}$), respectively. The absorption from 550 nm to 450 nm towards lower wavelengths in the entire spectrum (blue shift) corresponds to the absorption edge of the solids. The optical constant (band gap energy (E_g)) is extracted from UV–Visible DRS spectra. The fundamental indirect allowed transitions of $WO_{3-\delta}$ due to transition of O 2p electrons from the valance band to the W 5d conduction band.

The band gap energies (E_g) have been calculated using Kubelka–Munk (K–M) model as described below. The K–M model at any wavelength is given by

$$\frac{K}{S} = \frac{(1-R_\infty)^2}{2R_\infty} = F(R_\infty)$$

$F(R_\infty)$ is the so called remission or Kubelka–Munk function, where,

$$R_\infty = \frac{R\,\text{sample}}{R\,\text{standard}}$$

A graph is plotted between $[F(R_\infty)h\upsilon]^2$ vs $h\upsilon$ and the intercept value gives the band gap energy E_g [21] of the individual sample (see inset of Fig. 6). Thus, the band gap energies were estimated as 3.28

Table 1
Observed FT-IR wavenumbers (cm^{-1}) of as prepared $WO_3{\cdot}H_2O$ using EDTA as surfactant and annealed $W_{18}O_{49}$ samples.

$WO_3{\cdot}H_2O$	$W_{18}O_{49}$	Tentative assignments
3424 (vs)	3402 (m)	H–OH str.
2822 (vw)	2819 (vw)	Assy. CH_2 str.
1595 (vs)	1592 (s)	H–OH deformation vibration
1354 (w)	1352 (vw)	CH_2 wagging
819 (vs)	639 (vs)	W–O stretching
637 (vs)	816 (vs)	W–O stretching

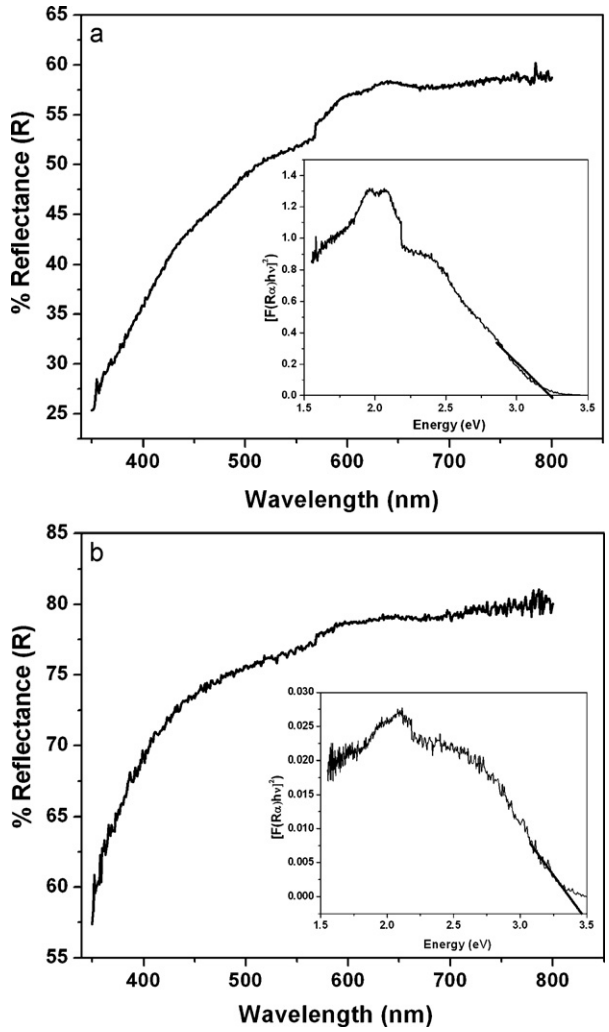

Fig. 6. UV–visible DRS spectra of EDTA assisted samples (a) $WO_3 \cdot H_2O$ (b) $W_{18}O_{49}$ (annealed at 600 °C for 6 h in air ambient). In both the cases, inset shows a plot between $[F(R_\infty)h\upsilon]^2$ vs $h\upsilon$ and the intercept value gives the band gap energy E_g of the individual sample.

and 3.47 eV for as prepared and annealed samples, respectively. Similar procedure was followed to calculate the band gap energies for $WO_3 \cdot H_2O$ and for $W_{17}O_{47}$ prepared without EDTA and the values were found to be 3.40 and 3.55 eV, respectively. This indicates the EDTA assisted samples have more optical conductivity than the surfactant free samples.

4. Conclusions

We have successfully synthesized $W_{17}O_{47}$ and $W_{18}O_{49}$ nanosheet like morphology by adopting a novel microwave irradiation method with and without using EDTA as surface modulator. The powder XRD results confirmed the as prepared samples in both the cases to be orthorhombic phase ($WO_3 \cdot H_2O$) and the annealed samples ($W_{17}O_{47}$ and $W_{18}O_{49}$) were indexed as monoclinc structures. TEM observation clearly demonstrated the role of EDTA in shaping surface morphology through formation of sheet like structure with the dimensions of 250 nm in length and 150 nm in width which served as building blocks for the formation of $W_{18}O_{49}$ bundles. The UV–Visible DRS analysis indicated the band gap energies of the EDTA assisted samples to be lighter than that of surfactant free samples. These observations suggest that the $W_{18}O_{49}$ nanosheets may be suitable for photo catalytic applications and the oxygen vacancy may be used to induce the changes in electrical properties.

Acknowledgments

The authors thank Dr. A. Thamizhavel, DCMP and MS, Tata Institute of Fundamental Research, Mumbai for his critical suggestions. Use of HRTEM facility of Unit on Nanoscience and Nanotechnology Initiative at IIT Delhi (Project No. SR/S5/NM-22/2004) of the Department of Science and Technology, Government of India is gratefully acknowledged.

References

[1] L.C. Chen, K.C. Ho, Electro. Acta 46 (2001) 2151–2158.
[2] L. Su, Z. Lu, J. Phys. Chem. Solids 59 (1998) 1175–1180.
[3] S.H. Lee, R. Deshpande, P.A. Parilla, K.M. Jones, B. To, A.H. Mahan, A.C. Dillon, Adv. Mater. 18 (2006) 763–766.
[4] Y.M. Zhao, Y.Q. Zhu, Sens. Actuators. B 137 (2009) 27–31.
[5] F. Kojin, M. Mori, Y. Noda, M. Inagaki, Apply. Catal. B-Environ. 78 (2008) 202–209.
[6] M. Saha, M.N. Banis, Y. Zhang, R. Li, X. Sun, M. Cai, F.T. Wagner, J. Power Sources 192 (2009) 330–335.
[7] M. Deepa, A.K. Srivastava, S.A. Agnihotry, Acta Mater. 54 (2006) 4583–4595.
[8] J. Ha, P. Muralidharan, D.K. Kim, J. Alloys Compd. 475 (2009) 446–451.
[9] N. Asim, S. Radiman, M.A.B. Yarmo Ameri, J. Appl. Sci. 6 (2009) 1424–1428.
[10] T. Kida, A. Nishiyama, M. Yuasa, K. Shimanoe, N. Yamazoe, Sens. Actuators B 135 (2009) 568–574.
[11] O. Nimittrakoolchai, S. Supothina, Mater. Chem. Phys. 112 (2008) 270–274.
[12] Y. Qin, M. Hu, J. Zhang, Sens. Actuators B 150 (2010) 339–345.
[13] M. Deepa, A.G. Joshi, A.K. Srivastava, S.M. Shivaprasad, S.A. Agnihotry, J. Electrochem. Soc. 153 (2006) 365–376.
[14] A. Wolcott, T.R. Kuykendall, W. Chen, S. Chen, J.Z. Zhang, J. Phys. Chem. 110 (2006) 25288–25396.
[15] T. Jesionowski, Powder Technol. 127 (2002) 56–65.
[16] I. Jimenex, J. Arbiol, A. Cornet, J. Ramon Morante, IEEE Sensors 2 (2002) 329–335.
[17] V. Von, D. Chemikerin, E. Rodel, A. Berlin, In situ bulk structural investigation of Mo_5O_{14}-type mixed metal oxide catalysts for partial oxidation reactions, Genehmigte Dissertation. Technical University, Berlin, 2006, pp. 16–19.
[18] J. Dattatray, V. Late Ranjit, K. Chandra Sekhar Rout, A. Mahendra, S. More Dilip, S. Joag, Appl. Phys. A 98 (2010) 751–756.
[19] E. Mauro, A. Teresa, A. Jordi, D. Raül, S. Pietro, R. Mornate Joan, Chem. Mater. 21 (2009) 5215–5221.
[20] J.D. Reyes, V.D. Garcia, A.P. Benitez, J.A.B. Lopez, Super.Y. Vacio 21 (2008) 12–17.
[21] A. Escobedo Morales, E. Sĩanchez Mora, U. Pal, Rev. Mex. Fis. 53 (2006) 18–22.